



Published in final edited form as:

*J Ultrasound Med.* 2007 September ; 26(9): 1181–1190.

## The Role of the Sagittal View of Ductal Arch in Identification of Fetuses with Conotruncal Anomalies using 4D Ultrasonography

Jimmy Espinoza, MD<sup>1,2</sup>, Roberto Romero, MD<sup>1,3</sup>, Juan Pedro Kusanovic, MD<sup>1</sup>, Francesca Gotsch, MD<sup>1</sup>, Wesley Lee, MD<sup>4</sup>, Luís F. Gonçalves, MD<sup>1,2</sup>, Mary Lou Schoen, RDMS<sup>2</sup>, Offer Erez<sup>1</sup>, and Sonia S. Hassan, MD<sup>2</sup>

<sup>1</sup> Perinatology Research Branch, NICHD, NIH, DHHS, Bethesda, Maryland and Detroit, Michigan

<sup>2</sup> Wayne State University, Department of Obstetrics and Gynecology, Detroit, Michigan

<sup>3</sup> Wayne State University, Center for Molecular Medicine and Genetics, Detroit, Michigan

<sup>4</sup> Division of Fetal Imaging, William Beaumont Hospital, Royal Oak, Michigan

### Abstract

**Objective**—Conotruncal anomalies represent one-fifth of all congenital heart defects (CHDs) detected in the fetus. However, the spatial relationship of the great vessels is incorrectly defined in about 20% of these cases. The sagittal view of the ductal arch is considered a standard ultrasonographic view in fetal echocardiography, and can be easily visualized using four-dimensional (4D) ultrasonography. This study was designed to determine the role of this ultrasonographic plane for the prenatal diagnosis of conotruncal anomalies.

**Methods**—We reviewed four-dimensional volume data sets, acquired with the spatiotemporal image correlation technique, from fetuses with and without confirmed conotruncal anomalies. The visualization rate of the sagittal view of the ductal arch was compared among groups using standardized multiplanar views.

**Results**—This study included 183 volume data sets from fetuses in the following groups: 1) normal echocardiography (n=130); 2) conotruncal anomalies (n=18); and 3) other CHDs (n=35). Volumes of poor image quality were excluded from analysis [8.2% (15/183)]. The visualization rate of the sagittal view of the ductal arch was significantly lower in fetuses with conotruncal anomalies [5.6% (1/18)] than that in fetuses without abnormalities [93.1% (108/116)] and that in fetuses with other CHDs [79.4% (27/34); P<0.01]. Absence of visualization of the sagittal view of the ductal arch was associated with a likelihood ratio of 9.44 (95% Confidence interval: 5.8–15.5) to have conotruncal anomalies.

**Conclusion**—The sagittal view of the ductal arch may play an important role in the screening and prenatal diagnosis of conotruncal anomalies in 4D ultrasonography.

### Keywords

Fetal echocardiography; ductus arteriosus; spatiotemporal; congenital heart disease; prenatal diagnosis; spatiotemporal image correlation; ductus arteriosus; three dimensional ultrasonography

## Introduction

Conotruncal anomalies are congenital heart defects (CHDs) characterized by abnormal development of the conotruncal septum, which include tetralogy of Fallot, absent pulmonary valve syndrome, double outlet right ventricle (DORV), transposition of the great arteries, malposition of the great arteries, and truncus arteriosus.<sup>1</sup> These anomalies represent one-fifth of all CHDs diagnosed prenatally.<sup>2,3</sup> However, difficulties in defining the spatial relationships of the great arteries may prevent an accurate diagnosis of the specific anomaly. Indeed, it has been reported that in about 20% of fetuses with prenatal diagnosis of conotruncal anomalies, the spatial relationship of the great vessels was incorrectly defined.<sup>1</sup> Although the accuracy in the prenatal diagnosis of these CHDs has improved,<sup>3</sup> the prenatal diagnosis of some outflow tract anomalies remains challenging.<sup>3,4</sup>

Accumulating evidence indicates that prenatal diagnosis of some congenital heart diseases, including transposition of the great arteries, hypoplastic left heart syndrome, and coarctation of the aorta, can reduce neonatal morbidity and mortality.<sup>5–8</sup> Thus, the development of novel approaches to examine the fetal heart using three-dimensional (3D) and four-dimensional (4D) ultrasonography may improve the detection rates and neonatal outcome of fetuses with conotruncal anomalies.

A detailed examination of the fetal heart has been proposed to include a long-axis view of the arterial duct<sup>9</sup> (sagittal view of the ductal arch). This ultrasonographic plane allows visualization of the right ventricle in continuity with the main pulmonary artery, pulmonary valve, ductus arteriosus, and descending aorta, as well as a transverse view of the ascending aorta (Figure 1). The sagittal view of the ductal arch can be easily obtained using 4D volume data sets of the fetal heart acquired with spatiotemporal image correction (STIC) by following the first two steps of a recently reported algorithm.<sup>10</sup> In that report, the sagittal view of ductal arch was visualized in 98.5% (192/195) of volume data sets from fetuses without CHDs and in 65% (13/20) of fetuses with CHDs.<sup>10</sup> The objective of this study was to determine the role of the sagittal view of the ductal arch in the prenatal diagnosis of conotruncal anomalies using 4D ultrasonography.

## Material and Methods

Four-dimensional volume data sets of the fetal heart were acquired with transverse sweeps through the fetal chest. Volume data sets (n=183) from fetuses in the following groups were included in the study: 1) normal heart (n=130); 2) conotruncal anomalies (n=18); and 3) other CHDs (n=35). Conotruncal anomalies were confirmed by prenatal or postnatal echocardiography or during autopsy. Examinations were performed with the STIC technique (Voluson 730 Expert, release BTO4, GE Healthcare, Milwaukee, WI) using hybrid mechanical and curved array transducers (RAB 4-8P, RAB 4-8L, RAB 2-5P, RAB 2-5L). The acquisition time ranged from 7.5 to 15 seconds and the angle of acquisition ranged between 20<sup>d</sup> and 40<sup>d</sup>, depending on fetal motion and gestational age. Patients were examined between 14 and 41 weeks of gestation (median 24.4 weeks; interquartile range: 20.9 to 28.9 weeks). All patients were enrolled in research protocols approved by the Institutional Review Board of the National Institute of Child Health and Human Development (NICHD/NIH/DHHS) and the Human Investigation Committees of both Wayne State University and William Beaumont Hospital. All women signed a written informed consent before participating in the study.

After removal of patient identifiers, ultrasonographic images were retrospectively reviewed offline using the 4D View software version 5.0 (General Electric Medical Systems, Kretztechnik, Zipf, Austria). The volume dataset considered by the investigator to be of highest quality was selected on the basis of the following characteristics: 1) the fetal spine was

positioned between three and nine o'clock positions, minimizing the possibility of shadowing from the ribs or spine; and 2) minimal or no motion artifacts were observed on the sagittal plane. B-mode ultrasonography was used to acquire all volume data sets. Volume data sets with poor image quality and those that did not contain the upper mediastinum were excluded from the study [8.2% (15/183)]. All volume data sets were reviewed by one operator who was not blinded to the results of the fetal echocardiography.

### Visualization of the Ductal Arch Plane

All volume data sets were analyzed using a multiplanar display, which allows simultaneous display of images in three orthogonal planes (Figure 2, panels A–C). The sagittal view of the ductal arch was visualized using the first two steps of a recently reported algorithm that allows for the simultaneous visualization of the standard planes for fetal echocardiography.<sup>10</sup> Briefly:

1. The volume data sets were adjusted to display the four-chamber view in panel A, where the fetal aorta was aligned with the crux of the heart in the vertical plane. The reference dot was positioned in the aorta, allowing the visualization of the coronal view of the descending aorta in panel C (Figure 2).
2. In panel C, the image was rotated to display the aorta in a vertical position, when necessary. This allowed for the visualization of the sagittal view of the ductal arch in panel B and the four chamber view in panel A (Figure 3).

### Statistical Analysis

Visualization rates of the sagittal view of the ductal arch were compared among groups using contingency tables and  $\chi^2$  test for independence. The likelihood ratio to have a conotruncal anomaly conferred by the absence of visualization of the sagittal view of the ductal arch was calculated.  $P < .05$  was considered significant. Statistical analysis was performed with SPSS 12.0 for Windows (SPSS, Chicago, IL).

### Results

The visualization rate of the sagittal view of the ductal arch was significantly lower in fetuses with conotruncal anomalies 5.6% (1/18), than that in fetuses without abnormalities [93.1% (108/116)] and those with other CHDs [79.4% (27/34);  $P < 0.01$ ]. Absence of visualization of the sagittal view of the ductal arch was associated with a likelihood ratio of 9.44 (95% Confidence interval: 5.8–15.5) to have a conotruncal anomaly.

Fetuses with the following conotruncal anomalies were included in the study: tetralogy of Fallot (n=6), transposition of the great arteries (n=4), DORV (n=4), tetralogy of Fallot with pulmonary atresia (pulmonary atresia with ventricular septal defect) (n=2), and truncus arteriosus (n=2). Among them the sagittal view of the ductal arch was visualized only in one case of DORV.

Among fetuses with CHDs other than conotruncal anomalies, the ductal arch plane was not visualized in seven fetuses with the following diagnoses: ventricular septal defects (n=2), coarctation of the aorta (n=2), atrioventricular canal (n=2), and Turner's syndrome (n=1). Of note, in one fetus with mediastinal displacement to the right, due to a large cystic adenomatoid malformation, the ductal arch was visualized using the proposed approach. This observation suggests that mechanical displacement of the heart may not necessarily change the spatial relationships of the ductal arch.

Specific abnormalities of the sagittal view of the ductal arch were consistently visualized in fetuses with conotruncal anomalies. Among fetuses with tetralogy of Fallot, the root of the

ductal arch was displaced downwards toward the aortic root (Figure 4). In patients with transposition of the great arteries, the main pulmonary artery and the ductus arteriosus were not visualized, (Figure 5), whereas in truncus arteriosus, the left atrium was displayed in the area corresponding to the aortic root in a normal sagittal view of the normal ductal arch (Figure 6). However, the limited number of cases in each diagnostic category prevents us from ascertaining whether these ultrasonographic patterns constitute stereotypical anomalies.

Among patients with CHDs other than conotruncal anomalies, a tortuous ductus arteriosus was visualized in fetuses with pulmonary valve atresia (Figure 7), and the ductus arteriosus and left pulmonary artery could be simultaneously visualized in a fetus with coarctation of aorta (Figure 8).

## Discussion

Our study demonstrates that the sagittal view of the ductal arch was not visualized in most fetuses with conotruncal defects using the proposed algorithm. Thus, examination of this ultrasonographic plane may play an important role in the prenatal diagnosis and screening for conotruncal anomalies with the use of 4D ultrasonography.

Two-dimensional (2D) ultrasonography relies on standard anatomic planes for a thorough examination of the fetal heart, including the four-chamber view, three-vessel and trachea view, the left and right outflow tracts, and the ductal arch plane.<sup>9,11–15</sup> More recently, it has been proposed that 3D and 4D ultrasonography with STIC can facilitate the visualization of these planes.<sup>16–63</sup> Thus, 3D and 4D fetal echocardiography could potentially reduce the operator dependency that occurs with 2D ultrasonography. The sagittal view of the ductal arch, also known as long-axis view of the arterial duct, is considered a standard plane for fetal echocardiography.<sup>9</sup> This ultrasonographic plane, easily visualized using 4D ultrasonography, played a central role in a recently reported algorithm for a thorough examination of the fetal heart.<sup>10</sup> Indeed, the three-vessel, five chamber and four chamber views were simultaneously visualized using perpendicular views to the ductal arch plane and tomographic ultrasonographic imaging.<sup>10</sup>

During early cardiogenesis, the conus and the truncus give origin to the great arteries and the subpulmonary infundibulum, respectively.<sup>64</sup> The truncus arteriosus is the most distal portion of the developing cardiac outflow tract, and its septation originates the ascending aorta and pulmonary trunk,<sup>65</sup> allowing the transition from a single- to a dual-series circulation.<sup>66</sup> Truncal endocardial cushions participate in the septation of the common truncus and in the formation of the aortic and pulmonary valves leaflets.<sup>64</sup> The conventional view is that septation of ventricles and outflow tracts must occur in tight coordination if the heart is to function properly, and a large proportion of CHDs are due to errors made during this complex process.<sup>65</sup>

Conotruncal anomalies, which represent one-fifth of all CHDs detected prenatally,<sup>2,3</sup> are frequently associated with chromosomal anomalies<sup>2,67–70</sup> and poor survival rates.<sup>2</sup> However, in about 20% of fetuses with these CHDs, the spatial relationship of the great vessels is incorrectly defined.<sup>1</sup> The observation that the ductal arch plane was not visualized in all but one fetus with conotruncal anomalies indicates that the inability to visualize the ductal arch using the proposed algorithm should raise the index of suspicion for such anomalies. Indeed, the inability to visualize a normal ductal arch plane with the proposed algorithm was associated with a nine-fold increase in the risk for a conotruncal anomaly.

The results of this study further demonstrate that 4D ultrasonography may provide important insight into the study of abnormal cardiac geometry in CHDs. We have used volume data sets obtained with 4D ultrasonography and STIC to examine the sagittal view of ductal arch.

However, the same approach could be applied to volume data sets obtained with 3D ultrasonography.

The ability to obtain the sagittal view of the ductal arch with two dimensional ultrasonography may depend on the operator experience and fetal position. In addition, the lack of simultaneous visualization of the orthogonal planes with two dimensional ultrasonography may increase the number of false-positive results if the sagittal view of the ductal arch is to be used for the prenatal diagnosis of conotruncal anomalies.

Limitations of this study include its retrospective nature and that the operator was not blinded to the results of the fetal echocardiography. Thus, prospective studies are required to determine the value of the proposed approach in the screening for conotruncal anomalies.

The multiplanar display of the sagittal view of the ductal arch proposed herein allows for simultaneous visualization of the four-chamber view of the heart and the sagittal view of the ductal arch, which may result in a more accurate prenatal diagnosis of specific conotruncal anomalies. Given its simplicity, we propose the use of this approach as a first step in the examination of three dimensional and four dimensional volume data she meets of the fetal heart. The lack of visualization of the sagittal view of the ductal arch should raise the index of suspicion for conotruncal anomalies.

#### Acknowledgements

This research was supported by the Intramural Research Program of the National Institute of Child Health and Human Development, NIH, DHHS.

#### Reference List

1. Tometzki AJ, Suda K, Kohl T, Kovalchin JP, Silverman NH. Accuracy of prenatal echocardiographic diagnosis and prognosis of fetuses with conotruncal anomalies. *J Am Coll Cardiol* 1999;33:1696–1701. [PubMed: 10334445]
2. Paladini D, Rustico M, Todros T, et al. Conotruncal anomalies in prenatal life. *Ultrasound Obstet Gynecol* 1996;8:241–246. [PubMed: 8916376]
3. Sivanandam S, Glickstein JS, Printz BF, et al. Prenatal diagnosis of conotruncal malformations: diagnostic accuracy, outcome, chromosomal abnormalities, and extracardiac anomalies. *Am J Perinatol* 2006;23:241–245. [PubMed: 16625498]
4. Smith RS, Comstock CH, Kirk JS, et al. Double-outlet right ventricle: an antenatal diagnostic dilemma. *Ultrasound Obstet Gynecol* 1999;14:315–319. [PubMed: 10623990]
5. Mahle WT, Clancy RR, McGaurn SP, Goin JE, Clark BJ. Impact of prenatal diagnosis on survival and early neurologic morbidity in neonates with the hypoplastic left heart syndrome. *Pediatrics* 2001;107:1277–1282. [PubMed: 11389243]
6. Franklin O, Burch M, Manning N, et al. Prenatal diagnosis of coarctation of the aorta improves survival and reduces morbidity. *Heart* 2002;87:67–69. [PubMed: 11751670]
7. Tworetzky W, McElhinney DB, Reddy VM, et al. Improved surgical outcome after fetal diagnosis of hypoplastic left heart syndrome. *Circulation* 2001;103:1269–1273. [PubMed: 11238272]
8. Bonnet D, Coltri A, Butera G, et al. Detection of transposition of the great arteries in fetuses reduces neonatal morbidity and mortality. *Circulation* 1999;99:916–918. [PubMed: 10027815]
9. Allan L. Technique of fetal echocardiography. *Pediatr Cardiol* 2004;25:223–233. [PubMed: 15360115]
10. Espinoza J, Kusanovic JP, Goncalves LF, et al. A novel algorithm for comprehensive fetal echocardiography using 4-dimensional ultrasonography and tomographic imaging. *J Ultrasound Med* 2006;25:947–956. [PubMed: 16870887]
11. Chaoui R. The examination of the normal fetal heart using two-dimensional fetal echocardiography. *2003*:141–149.

12. Carvalho JS, Mavrides E, Shinebourne EA, Campbell S, Thilaganathan B. Improving the effectiveness of routine prenatal screening for major congenital heart defects. *Heart* 2002;88:387–391. [PubMed: 12231598]
13. Bromley B, Estroff JA, Sanders SP, et al. Fetal echocardiography: accuracy and limitations in a population at high and low risk for heart defects. *Am J Obstet Gynecol* 1992;166:1473–1481. [PubMed: 1595802]
14. Benacerraf BR. Sonographic detection of fetal anomalies of the aortic and pulmonary arteries: value of four-chamber view vs direct images. *AJR Am J Roentgenol* 1994;163:1483–1489. [PubMed: 7992752]
15. Comstock CH. What to expect from routine midtrimester screening for congenital heart disease. *Semin Perinatol* 2000;24:331–342. [PubMed: 11071374]
16. Deng J, Gardener JE, Rodeck CH, Lees WR. Fetal echocardiography in three and four dimensions. *Ultrasound Med Biol* 1996;22:979–986. [PubMed: 9004421]
17. Meyer-Wittkopf M, Cook A, McLennan A, et al. Evaluation of three-dimensional ultrasonography and magnetic resonance imaging in assessment of congenital heart anomalies in fetal cardiac specimens. *Ultrasound Obstet Gynecol* 1996;8:303–308. [PubMed: 8978001]
18. Nelson TR, Pretorius DH, Sklansky M, Hagen-Ansert S. Three-dimensional echocardiographic evaluation of fetal heart anatomy and function: acquisition, analysis, and display. *J Ultrasound Med* 1996;15:1–9. [PubMed: 8667477]
19. Zosmer N, Jurkovic D, Jauniaux E, et al. Selection and identification of standard cardiac views from three-dimensional volume scans of the fetal thorax. *J Ultrasound Med* 1996;15:25–32. [PubMed: 8667480]
20. Chang FM, Hsu KF, Ko HC, et al. Fetal heart volume assessment by three-dimensional ultrasound. *Ultrasound Obstet Gynecol* 1997;9:42–48.
21. Sklansky MS, Nelson TR, Pretorius DH. Usefulness of gated three-dimensional fetal echocardiography to reconstruct and display structures not visualized with two-dimensional imaging. *Am J Cardiol* 1997;80:665–668. [PubMed: 9295008]
22. Levental M, Pretorius DH, Sklansky MS, et al. Three-dimensional ultrasonography of normal fetal heart: comparison with two-dimensional imaging. *J Ultrasound Med* 1998;17:341–348. [PubMed: 9623470]
23. Nelson TR. Three-dimensional fetal echocardiography. *Prog Biophys Mol Biol* 1998;69:257–272. [PubMed: 9785942]
24. Sklansky MS, Nelson TR, Pretorius DH. Three-dimensional fetal echocardiography: gated versus nongated techniques. *J Ultrasound Med* 1998;17:451–457. [PubMed: 9669304]
25. Sklansky MS, Nelson T, Strachan M, Pretorius D. Real-time three-dimensional fetal echocardiography: initial feasibility study. *J Ultrasound Med* 1999;18:745–752. [PubMed: 10547106]
26. Guerra FA, Isla AI, Aguilar RC, Fritz EG. Use of free-hand three-dimensional ultrasound software in the study of the fetal heart. *Ultrasound Obstet Gynecol* 2000;16:329–334. [PubMed: 11169308]
27. Levi S, Cos-Sanchez T. Fetal echocardiography volume mode (3 dimensions). *J Gynecol Obstet Biol Reprod (Paris)* 2000;29:261–263. [PubMed: 10804367]
28. Meyer-Wittkopf M, Rappe N, Sierra F, Barth H, Schmidt S. Three-dimensional (3-D) ultrasonography for obtaining the four and five-chamber view: comparison with cross-sectional (2-D) fetal sonographic screening. *Ultrasound Obstet Gynecol* 2000;15:397–402. [PubMed: 10976481]
29. Scharf A, Geka F, Steinborn A, et al. 3D real-time imaging of the fetal heart. *Fetal Diagn Ther* 2000;15:267–274. [PubMed: 10971079]
30. Bega G, Kuhlman K, Lev-Toaff A, Kurtz A, Wapner R. Application of three-dimensional ultrasonography in the evaluation of the fetal heart. *J Ultrasound Med* 2001;20:307–313. [PubMed: 11316308]
31. Deng J, Yates R, Birkett AG, et al. Online motion-gated dynamic three-dimensional echocardiography in the fetus--preliminary results. *Ultrasound Med Biol* 2001;27:43–50. [PubMed: 11295269]
32. Meyer-Wittkopf M, Cooper S, Vaughan J, Sholler G. Three-dimensional (3D) echocardiographic analysis of congenital heart disease in the fetus: comparison with cross-sectional (2D) fetal echocardiography. *Ultrasound Obstet Gynecol* 2001;17:485–492. [PubMed: 11422968]

33. Meyer-Wittkopf M, Cole A, Cooper SG, Schmidt S, Sholler GF. Three-dimensional quantitative echocardiographic assessment of ventricular volume in healthy human fetuses and in fetuses with congenital heart disease. *J Ultrasound Med* 2001;20:317–327. [PubMed: 11316309]
34. Michailidis GD, Simpson JM, Karidas C, Economides DL. Detailed three-dimensional fetal echocardiography facilitated by an Internet link. *Ultrasound Obstet Gynecol* 2001;18:325–328. [PubMed: 11778990]
35. Arzt W, Tulzer G, Aigner M. Real time 3D sonography of the normal fetal heart--clinical evaluation. *Ultraschall Med* 2002;23:388–391. [PubMed: 12514755]
36. Deng J, Yates R, Sullivan ID, et al. Dynamic three-dimensional color Doppler ultrasound of human fetal intracardiac flow. *Ultrasound Obstet Gynecol* 2002;20:131–136.
37. Deng J, Sullivan ID, Yates R, et al. Real-time three-dimensional fetal echocardiography--optimal imaging windows. *Ultrasound Med Biol* 2002;28:1099–1105. [PubMed: 12401378]
38. Deng J, Richards R. Dynamic three-dimensional gray-scale and color Doppler ultrasound of the fetal heart for dynamic diagnosis. *Ultrasound Obstet Gynecol* 2002;20:209. [PubMed: 12153679]
39. DeVore GR, Falkensammer P, Sklansky MS, Platt LD. Spatio-temporal image correlation (STIC): new technology for evaluation of the fetal heart. *Ultrasound Obstet Gynecol* 2003;22:380–387. [PubMed: 14528474]
40. Goncalves LF, Lee W, Chaiworapongsa T, et al. Four-dimensional ultrasonography of the fetal heart with spatiotemporal image correlation. *Am J Obstet Gynecol* 2003;189:1792–1802. [PubMed: 14710117]
41. Herberg U, Goldberg H, Breuer J. Dynamic free-hand three-dimensional fetal echocardiography gated by cardiocography. *Ultrasound Obstet Gynecol* 2003;22:493–502. [PubMed: 14618663]
42. Jurgens J, Chaoui R. Three-dimensional multiplanar time-motion ultrasound or anatomical M-mode of the fetal heart: a new technique in fetal echocardiography. *Ultrasound Obstet Gynecol* 2003;21:119–123. [PubMed: 12601830]
43. Maulik D, Nanda NC, Singh V, et al. Live three-dimensional echocardiography of the human fetus. *Echocardiography* 2003;20:715–721. [PubMed: 14641376]
44. Meyer-Wittkopf M, Hofbeck M. Two- and three-dimensional echocardiographic analysis of congenital heart disease in the fetus. *Herz* 2003;28:240–249. [PubMed: 12756481]
45. Sklansky M. New dimensions and directions in fetal cardiology. *Curr Opin Pediatr* 2003;15:463–471. [PubMed: 14508293]
46. Vinals F, Poblete P, Giuliano A. Spatio-temporal image correlation (STIC): a new tool for the prenatal screening of congenital heart defects. *Ultrasound Obstet Gynecol* 2003;22:388–394. [PubMed: 14528475]
47. Abuhamad A. Automated multiplanar imaging: a novel approach to ultrasonography. *J Ultrasound Med* 2004;23:573–576. [PubMed: 15154522]
48. Acar P, Dulac Y, Taktak A, Villaceque M. Real time 3D echocardiography in congenital heart disease. *Arch Mal Coeur Vaiss* 2004;97:472–478. [PubMed: 15214550]
49. Bhat AH, Corbett VN, Liu R, et al. Validation of volume and mass assessments for human fetal heart imaging by 4-dimensional spatiotemporal image correlation echocardiography: in vitro balloon model experiments. *J Ultrasound Med* 2004;23:1151–1159. [PubMed: 15328429]
50. Bhat AH, Corbett V, Carpenter N, et al. Fetal ventricular mass determination on three-dimensional echocardiography: studies in normal fetuses and validation experiments. *Circulation* 2004;110:1054–1060. [PubMed: 15326076]
51. Brekke S, Tegnander E, Torp HG, Eik-Nes SH. Tissue Doppler gated (TDOG) dynamic three-dimensional ultrasound imaging of the fetal heart. *Ultrasound Obstet Gynecol* 2004;24:192–198. [PubMed: 15287059]
52. Chaoui R, Hoffmann J, Heling KS. Three-dimensional (3D) and 4D color Doppler fetal echocardiography using spatio-temporal image correlation (STIC). *Ultrasound Obstet Gynecol* 2004;23:535–545. [PubMed: 15170792]
53. DeVore GR, Polanco B, Sklansky MS, Platt LD. The 'spin' technique: a new method for examination of the fetal outflow tracts using three-dimensional ultrasound. *Ultrasound Obstet Gynecol* 2004;24:72–82. [PubMed: 15229920]

54. Espinoza J, Goncalves LF, Lee W, et al. The use of the minimum projection mode in 4-dimensional examination of the fetal heart with spatiotemporal image correlation. *J Ultrasound Med* 2004;23:1337–1348. [PubMed: 15448324]
55. Goncalves LF, Espinoza J, Lee W, Mazor M, Romero R. Three- and four-dimensional reconstruction of the aortic and ductal arches using inversion mode: a new rendering algorithm for visualization of fluid-filled anatomical structures. *Ultrasound Obstet Gynecol* 2004;24:696–698. [PubMed: 15521086]
56. Goncalves LF, Espinoza J, Romero R, et al. A systematic approach to prenatal diagnosis of transposition of the great arteries using 4-dimensional ultrasonography with spatiotemporal image correlation. *J Ultrasound Med* 2004;23:1225–1231. [PubMed: 15328439]
57. Goncalves LF, Romero R, Espinoza J, et al. Four-dimensional ultrasonography of the fetal heart using color Doppler spatiotemporal image correlation. *J Ultrasound Med* 2004;23:473–481. [PubMed: 15098864]
58. Sklansky MS, DeVore GR, Wong PC. Real-time 3-dimensional fetal echocardiography with an instantaneous volume-rendered display: early description and pictorial essay. *J Ultrasound Med* 2004;23:283–289. [PubMed: 14992367]
59. Espinoza J, Goncalves LF, Lee W, Mazor M, Romero R. A novel method to improve prenatal diagnosis of abnormal systemic venous connections using three- and four-dimensional ultrasonography and 'inversion mode'. *Ultrasound Obstet Gynecol* 2005;25:428–434. [PubMed: 15846761]
60. Goncalves LF, Espinoza J, Lee W, et al. A new approach to fetal echocardiography: digital casts of the fetal cardiac chambers and great vessels for detection of congenital heart disease. *J Ultrasound Med* 2005;24:415–424. [PubMed: 15784759]
61. Herberg U, Goldberg H, Breuer J. Three- and four-dimensional freehand fetal echocardiography: a feasibility study using a hand-held Doppler probe for cardiac gating. *Ultrasound Obstet Gynecol* 2005;25:362–371. [PubMed: 15761914]
62. Vinals F, Mandujano L, Vargas G, Giuliano A. Prenatal diagnosis of congenital heart disease using four-dimensional spatio-temporal image correlation (STIC) telemedicine via an Internet link: a pilot study. *Ultrasound Obstet Gynecol* 2005;25:25–31. [PubMed: 15593355]
63. Yagel S, Valsky DV, Messing B. Detailed assessment of fetal ventricular septal defect with 4D color Doppler ultrasound using spatio-temporal image correlation technology. *Ultrasound Obstet Gynecol* 2005;25:97–98. [PubMed: 15690557]
64. Restivo A, Piacentini G, Placidi S, Saffirio C, Marino B. Cardiac outflow tract: a review of some embryogenetic aspects of the conotruncal region of the heart. *Anat Rec A Discov Mol Cell Evol Biol* 2006;288:936–943. [PubMed: 16892424]
65. Larsen WJ. *Development of the Heart* 1993:131–165.
66. Sugishita Y, Watanabe M, Fisher SA. The development of the embryonic outflow tract provides novel insights into cardiac differentiation and remodeling. *Trends Cardiovasc Med* 2004;14:235–241. [PubMed: 15451515]
67. Lurie IW, Kappetein AP, Loffredo CA, Ferencz C. Non-cardiac malformations in individuals with outflow tract defects of the heart: the Baltimore-Washington Infant Study (1981–1989). *Am J Med Genet* 1995;59:76–84. [PubMed: 8849016]
68. Cuneo BF. 22q11.2 deletion syndrome: DiGeorge, velocardiofacial, and conotruncal anomaly face syndromes. *Curr Opin Pediatr* 2001;13:465–472. [PubMed: 11801894]
69. Stewart DR, Huang A, Faravelli F, et al. Subtelomeric deletions of chromosome 9q: a novel microdeletion syndrome. *Am J Med Genet A* 2004;128:340–351. [PubMed: 15264279]
70. Beauchesne LM, Warnes CA, Connolly HM, et al. Prevalence and clinical manifestations of 22q11.2 microdeletion in adults with selected conotruncal anomalies. *J Am Coll Cardiol* 2005;45:595–598. [PubMed: 15708709]



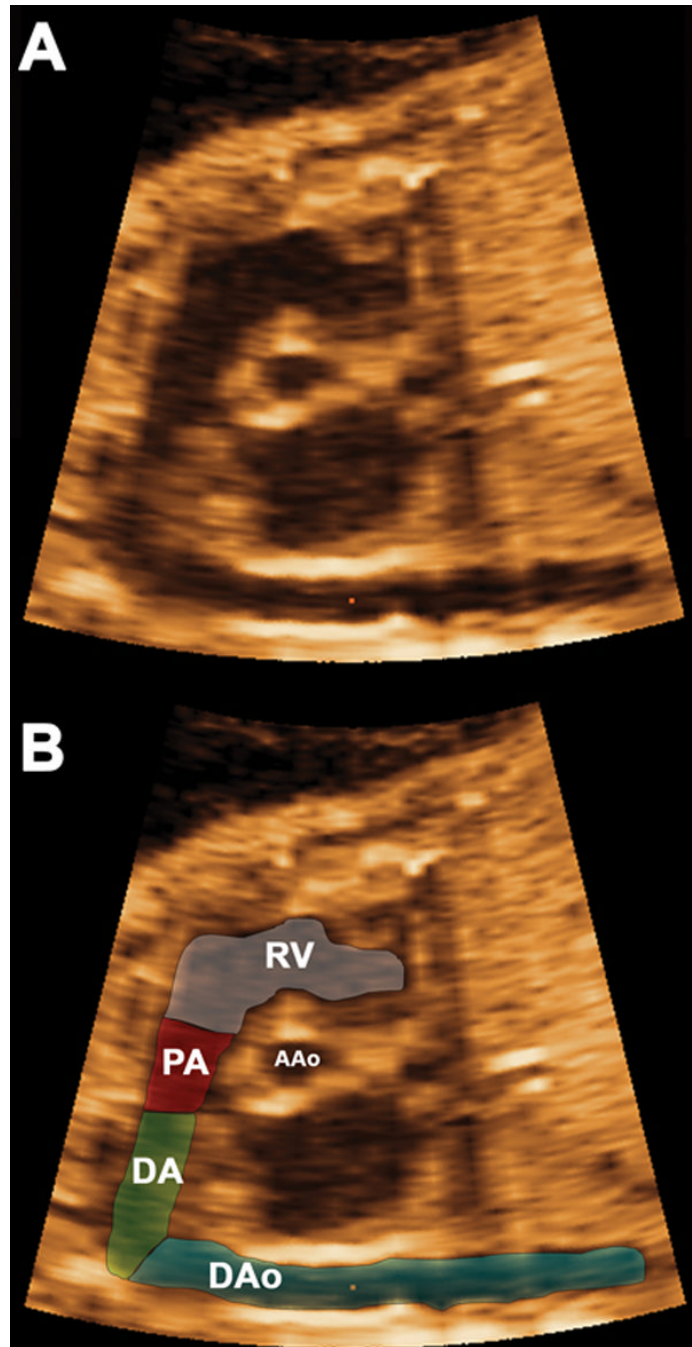


**Figure 1.** The components of the sagittal view of the ductal arch (Figure 1A) as determined by the multiplanar display are displayed in Figure 1B, including: right ventricular outlet (RV), main pulmonary artery (PA), ductus arteriosus (DA), descending aorta (DAo), and a cross-section of the ascending aorta (AAo).

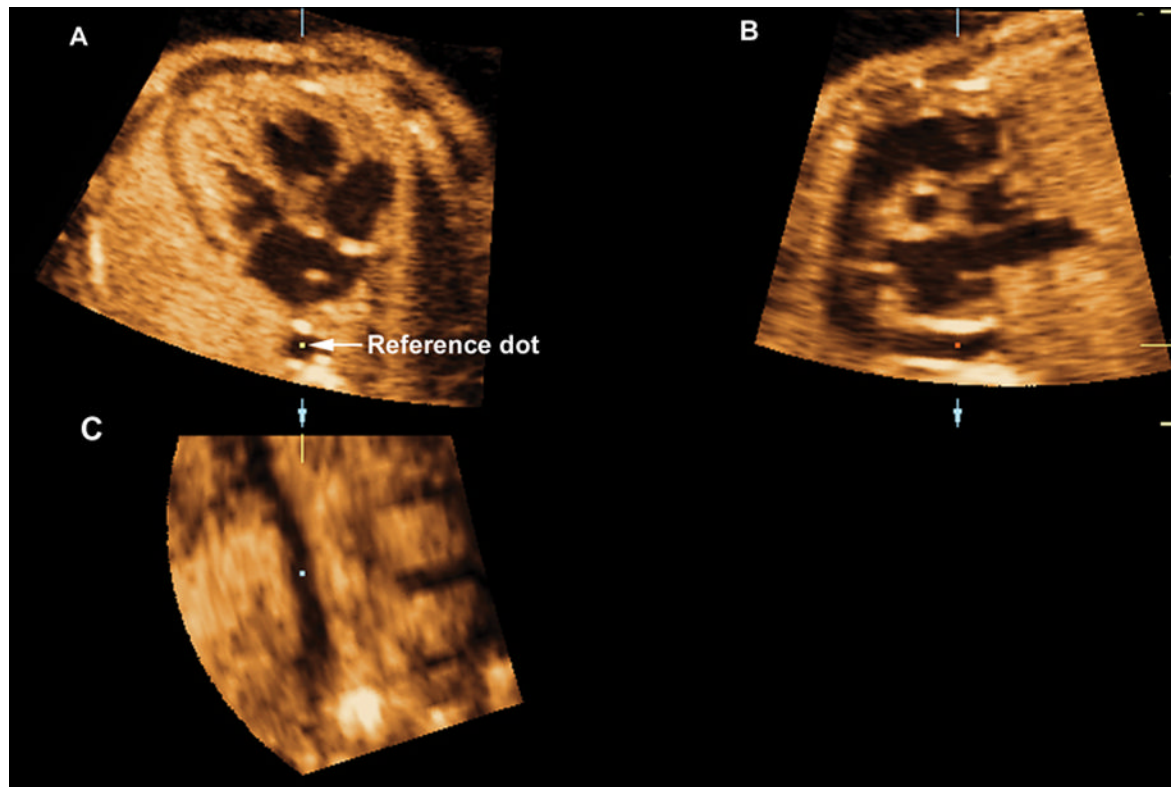


**Figure 2.**

Volume data sets were adjusted to display the four chamber view in panel A, where the fetal aorta was aligned with the crux of the heart in the vertical plane. The reference dot was positioned in the aorta allowing the visualization of the coronal view of the descending aorta in panel C. Ao indicates aorta; Da, ductus arteriosus; D Ao, descending aorta; LV, left ventricular; PA, pulmonary artery; and RV, right ventricular.

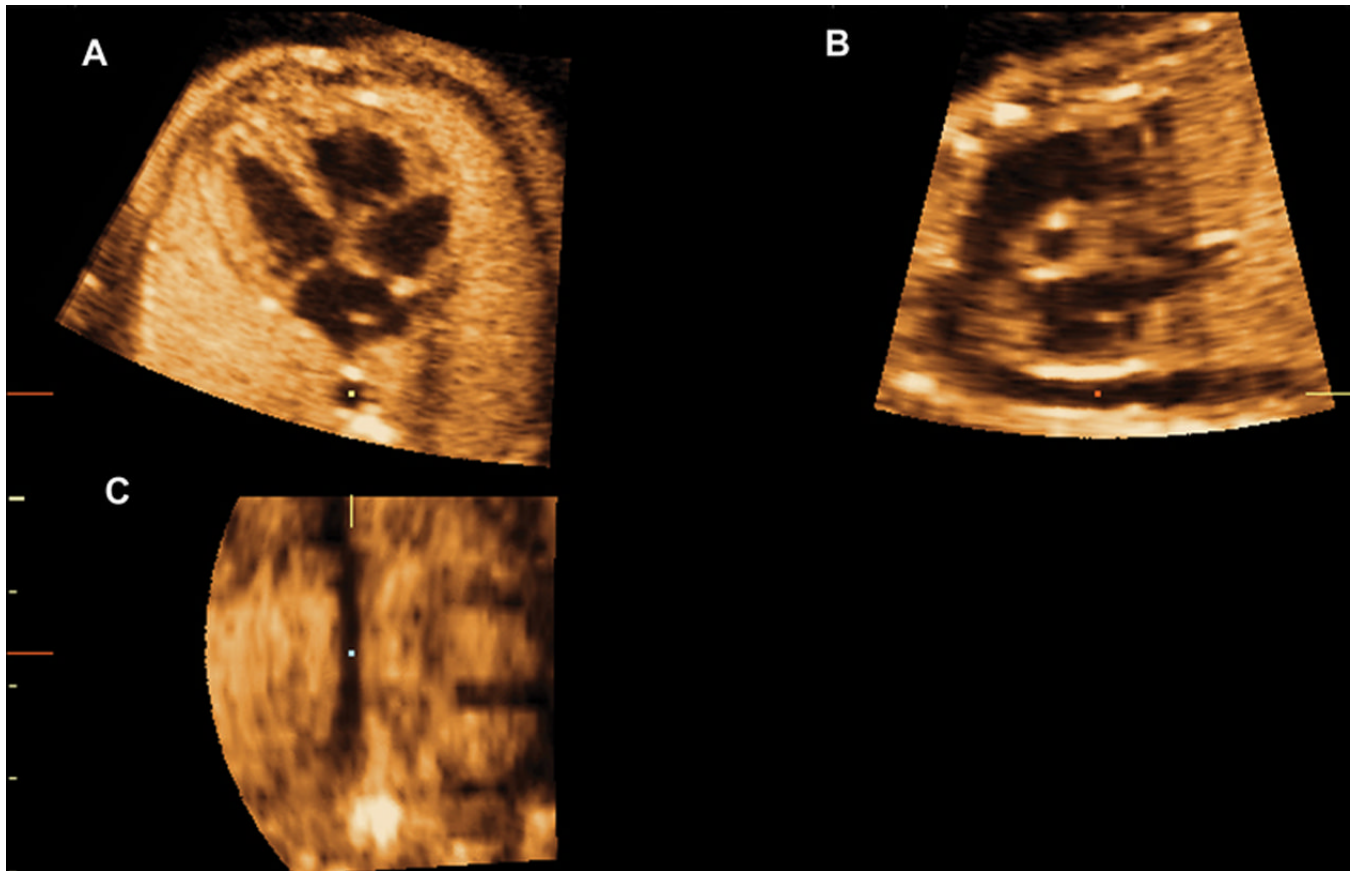


**Figure 3.** In panel C, the image was rotated to display the aorta in a vertical position, when necessary. This allowed for the visualization of the longitudinal view of the ductal arch in panel B. Ao indicates aorta; Da, ductus arteriosus; D Ao, descending aorta; LV, left ventricle; PA, pulmonary artery; and RV, right ventricle.

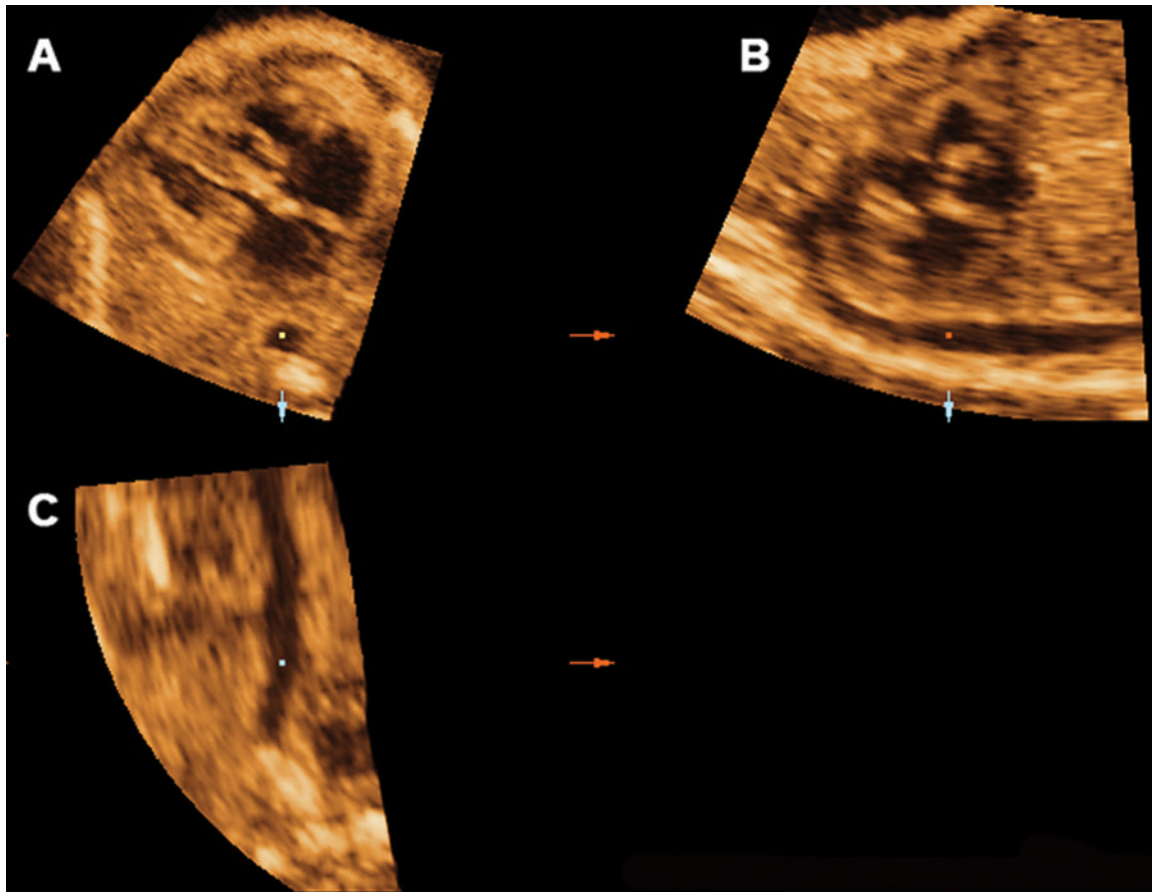


**Figure 4.** Muliplanar display of the sagittal view of the ductal arch in a fetus with tetralogy of fallot. The root of the ductal arch was displaced downwards, toward the aortic root. Ao indicates aorta; Da, ductus arteriosus; D Ao, descending aorta; LV, left ventricle; PA, pulmonary artery; and RV, right ventricle.

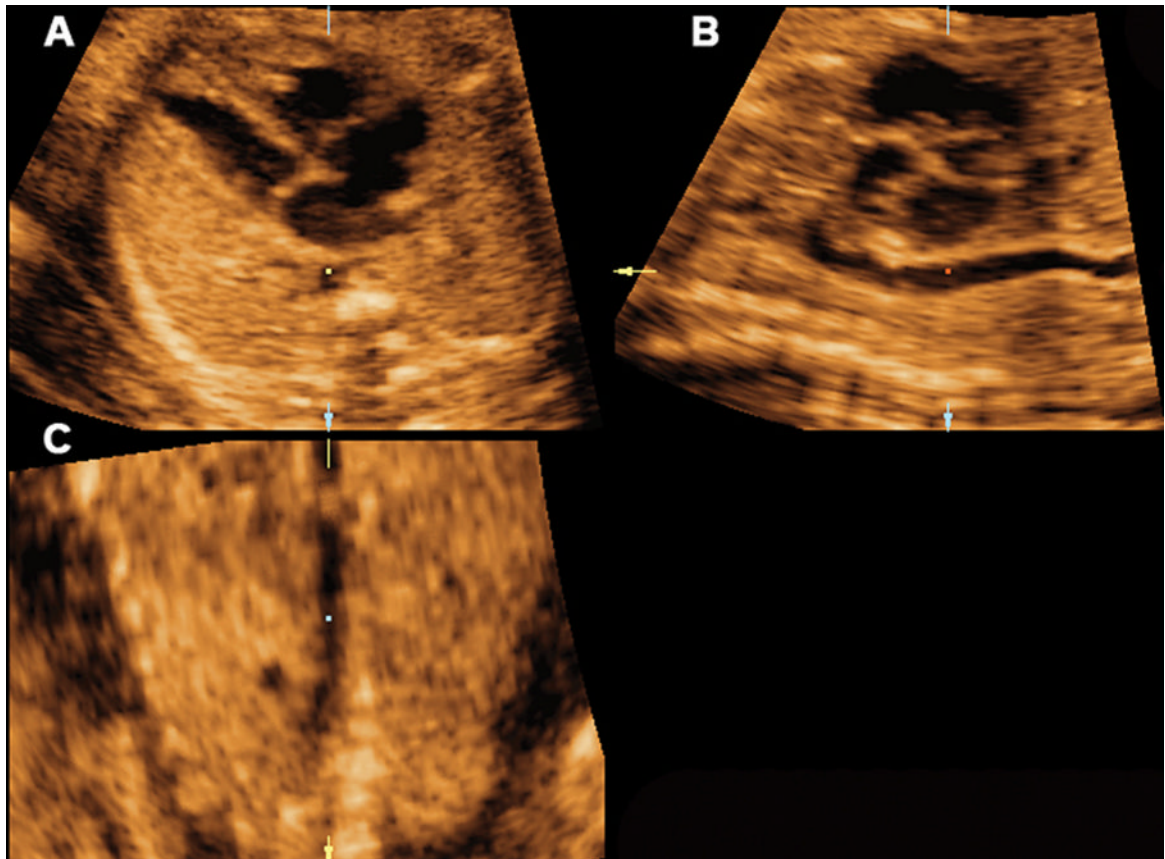


**Figure 5.** Muliplanar display of the sagittal view of the ductal arch in a fetus with transposition of the great arteries where the main pulmonary artery and the ductus arteriosus were not visualized. Ao indicates aorta; Da, ductus arteriosus; D Ao, descending aorta; LV, left ventricle; PA, pulmonary artery; and RV, right ventricle.

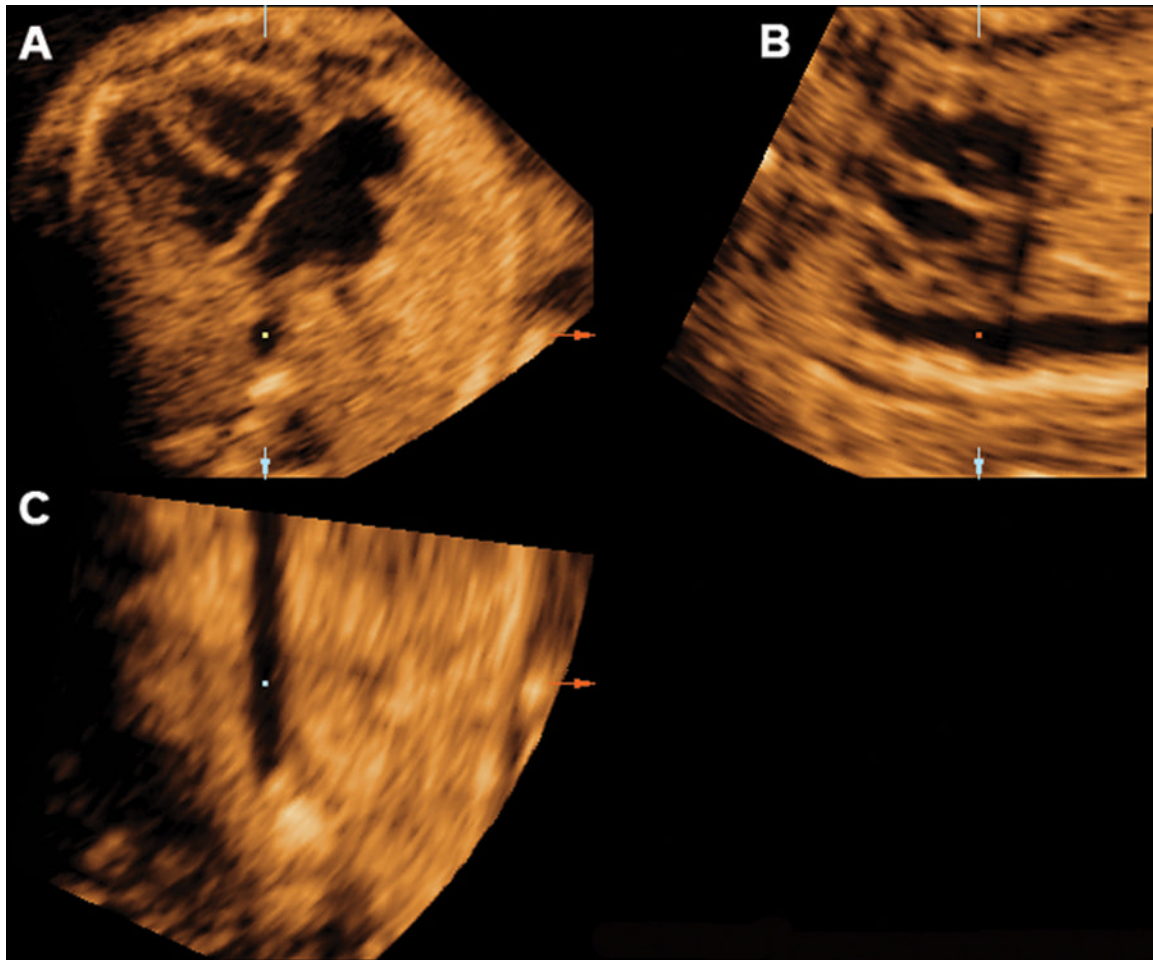


**Figure 6.**

Mutiplanar display of the sagittal view of the ductal arch in a fetus with truncus arteriosus. The left atrium was displayed in the area corresponding to the aortic root in a normal sagittal view of the ductal arch. Ao indicates aorta; Da, ductus arteriosus; D Ao, descending aorta; LV, left ventricle; PA, pulmonary artery; and RV, right ventricle.

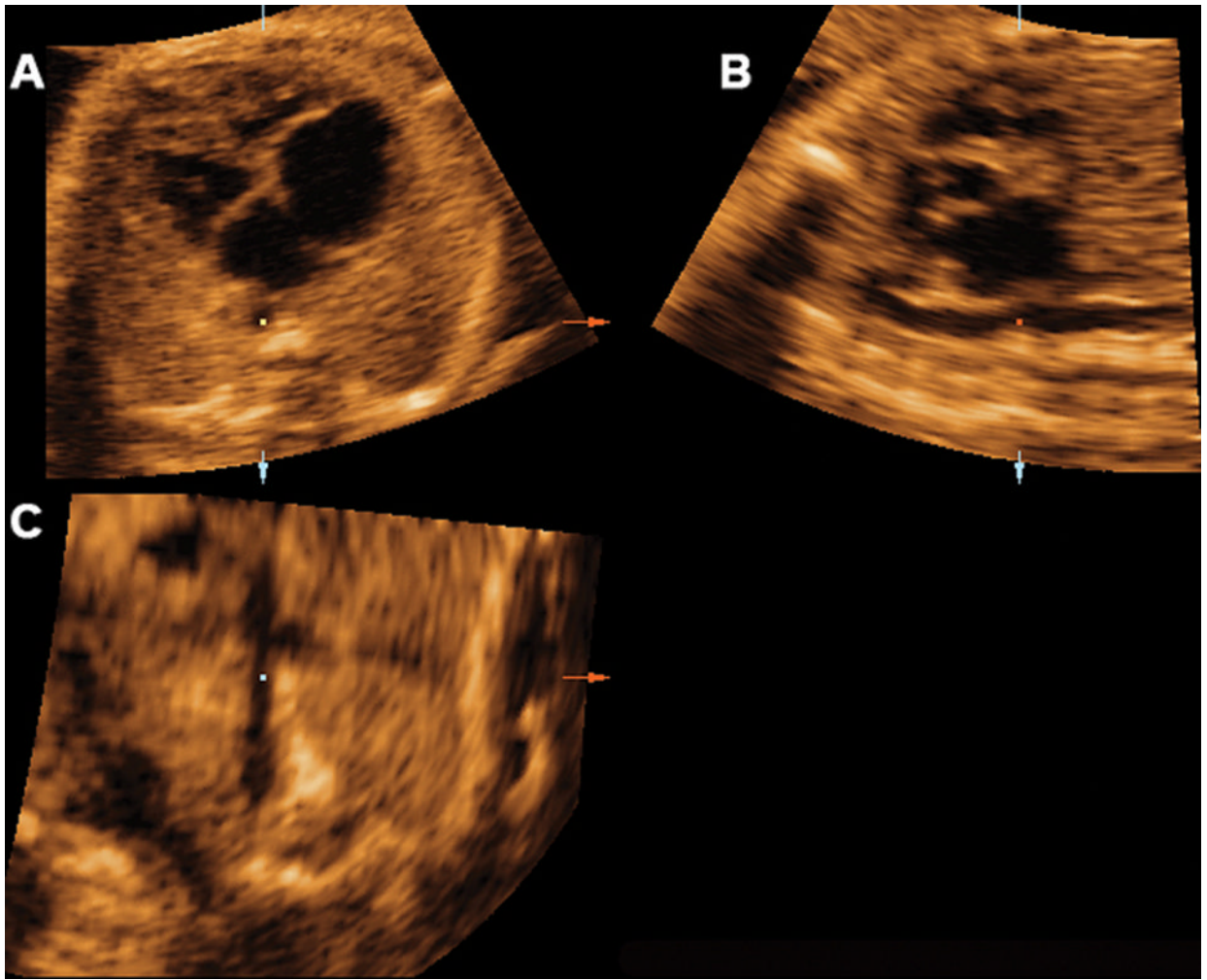


**Figure 7.** Muliplanar display of the sagittal view of the ductal arch in a fetus with pulmonary atresia, where a tortuous ductus arteriosus is visualized. Ao indicates aorta; Da, ductus arteriosus; D Ao, descending aorta; LV, left ventricle; PA, pulmonary artery; and RV, right ventricle.

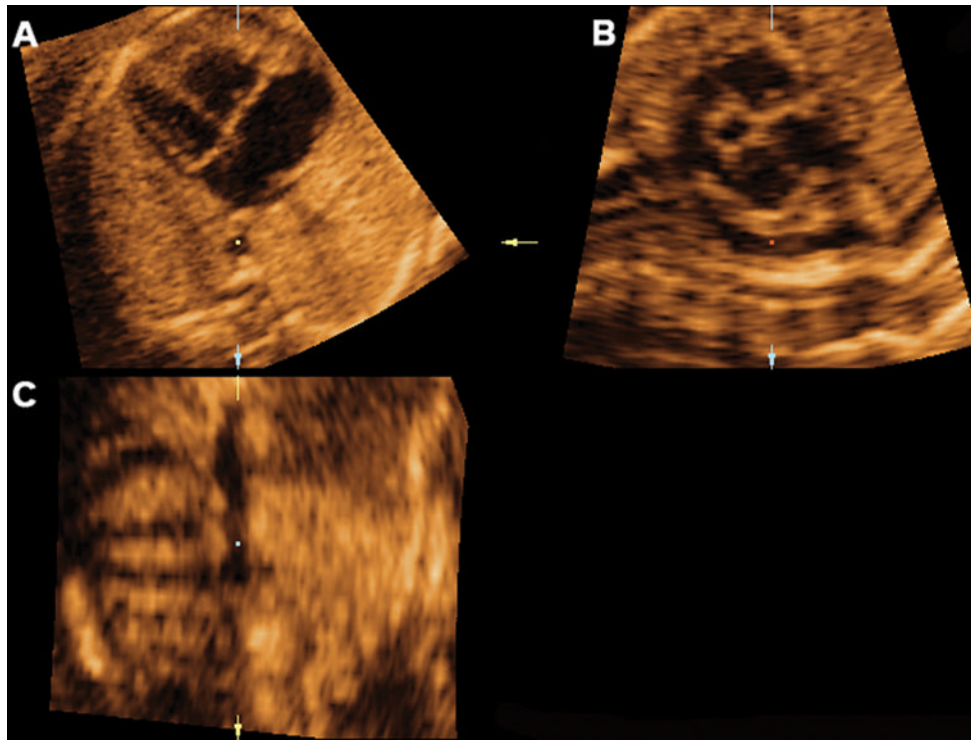


**Figure 8.** Mutiplanar display of the sagittal view of the ductal arch in a fetus with coarctation of the aorta, where the ductus arteriosus and left pulmonary artery can be visualized. Ao indicates aorta; Da, ductus arteriosus; D Ao, descending aorta; LV, left ventricle; PA, pulmonary artery; and RV, right ventricle.